Covalent complex of microperoxidase with a 21-residue synthetic peptide as a maquette for low-molecular-mass redox proteins

Rodolfo IPPOLITI*[1], Alessandra PICCIAU*, Roberto SANTUCCI†, Giovanni ANTONINI‡, Maurizio BRUNORI* and Graziella RANGHINO§

*Department of Biochemical Sciences 'A. Rossi-Fanelli', University of Rome La Sapienza, P. le Aldo Moro 5, 00185 Rome, Italy,
†Department of Experimental Medicine and Biochemical Sciences, University of Rome Tor Vergata, Via di Tor Vergata 135, 00133 Rome, Italy,
‡Department of Pure and Applied Biology, University of L'Aquila, Via Vetoio, Coppito, 67010 L'Aquila, Italy, and §EniChem, Guido Donegani Institute, Via G. Fauser 4, 28100 Novara, Italy

Here we report the structural and functional characterization of a covalent complex (MKP) obtained by cross-linking microperoxidase (Mp), the haem-undecapeptide obtained by the peptic digestion of cytochrome *c*, with a 21-residue synthetic peptide (P21) analogous to the S-peptide of the RNase A. The covalent complex has been prepared by introducing a disulphide bond between Cys-1 of P21 and Lys-13 of Mp, previously modified with a thiol-containing reagent. On formation of the complex (which is a monomer), the helical content of P21 increases significantly. The results obtained indicate that His-13 of P21 co-ordinates to the sixth co-ordination position of the haem iron, thus leading to the formation of a complex characterized by an equilibrium between an 'open' and a 'closed' structure, as confirmed by molecular dynamics simulations. Under acidic pH conditions, where His-13 of P21 is loosely bound to the haem iron ('open' conformation), MKP displays appreciable, quasi-reversible electrochemical activity; in contrast, at neutral pH ('closed' conformation) electrochemical behaviour is negligible, indicating that P21 interferes with the electron-transfer properties typical of Mp. On the whole, MKP is a suitable starting material for building a miniature haem system, with interesting potential for application to biosensor technology.

INTRODUCTION

Studies of complexes between haem and polypeptides, obtained either by enzymic digestion or by synthesis *de novo*, are of current interest as tools for understanding not only the role of the protein matrix in controlling the chemistry of the haem moiety but also the folding of the polypeptide. As pointed out by several authors [1], the advantage of designing and synthesizing haem–polypeptide complexes is related to the great potential afforded by chemical synthesis of the peptide, which allows engineering *de novo* and the use of non-natural amino acids if necessary. Within this perspective, we have synthesized and characterized a covalent complex between a synthetic peptide 21 residues long (P21) and microperoxidase (Mp).

Mp, the haem-containing undecapeptide obtained by peptic digestion of cytochrome *c* [2,3], is an interesting starting material for the construction of miniature haem complexes. The haem is covalently bound to the polypeptide chain through thioether bonds (involving two Cys residues and the haem vinyl groups) and one His residue is co-ordinated to the haem iron on the 'proximal side', as in the parent macromolecule. The structural and redox properties of Mp have been investigated [3–6]. We felt that this system provides a good opportunity to mimic the behaviour of the parent macromolecule from the bottom up, and to investigate the haem when it is relatively unshielded but still soluble in aqueous medium over a reasonably wide pH range. Among other applications [7], Mp has been introduced as a 'solid-state' promoter in the electrochemistry of metalloproteins [8,9]; the results indicated that Mp is an efficient, non-invasive promoter that can be employed successfully in voltammetric analysis of metalloproteins. These results stimulated further investigations to synthesize more complex systems that, by coupling electrochemical efficiency to good biological selectivity, might find applications in biosensor technology.

Our strategy has been to prepare and characterize complexes of Mp with synthetic peptides that are 'targeted' to the sixth co-ordination position of the haem iron by containing one His, given that imidazole is known [3] to bind to Mp. To achieve novel haem complexes with a likely degree of structural complexity demands the design of suitable peptides. This choice is not obvious because short peptides (10–20 residues) have a strong tendency to aggregate in water and are often randomly coiled. Interesting exceptions are two peptides of RNase A, i.e. the C-peptide (residues 1–13 of RNase-A) and the S-peptide (residues 1–20 of RNase A) [10–13], which display appreciable solubility and partial α-helical secondary structure in water at 4 °C. Moreover these two peptides are likely to form a co-ordination complex with Mp in view of the presence in their sequence of one His that might co-ordinate to the haem iron via its imidazole side chain.

Recently we have characterized the 1:1 co-ordination complex formed by Mp with a synthetic analogue of the C-peptide [14]; the results indicated that stabilization of the complex is due primarily (but not exclusively) to the binding of His-12 of the 13-mer at the sixth co-ordination position of the haem iron of Mp. This complex was shown to have appreciable α-helical content and good electrochemical activity. Here we report the structural and functional characterization of a covalent complex (called the MKP complex) obtained by cross-linking Mp to a suitably modified synthetic analogue of the S-peptide composed of 21 residues. The chemical structure of MKP is shown in Figure 1, where the numbers 11–21 in the haem peptide refer to the

Abbreviations used: MKP, covalent complex of microperoxidase with P21 synthetic peptide; Mp, microperoxidase; SPDP, *N*-succinimidyl-3-(2-pyridyldithio)propionate.

[1] To whom correspondence should be addressed.

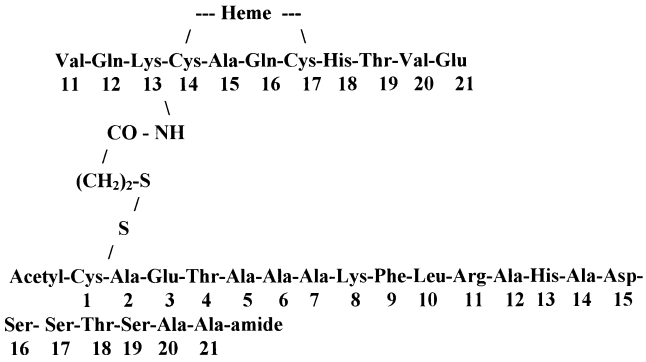

Figure 1 Schematic chemical structure of MKP

For details, refer to text.

position of residues in native cytochrome *c*. The MKP complex contains a cross-link between Lys-13 of Mp and Cys-1 of P21, is stable over the pH range 4–8 and has a significant degree of α-helical structure (approx. 30 % at neutral pH). Moreover we show that His-13 of P21 is co-ordinated to the iron atom of Mp in the Fe(III) oxidation state, leading to a 'closed structure' in equilibrium with an 'open structure'; a model featuring these two configurations of MKP has been simulated by molecular dynamics simulations. Switching the pH from acid to neutral conditions might trigger the transition from 'open' to 'closed'; moreover MKP displays an appreciable electrochemical activity only under acidic conditions, indicating that P21 (interacting with Mp at both acid and neutral pH values) interferes with the electron transfer activity of Mp at pH 7.0, probably owing to a decreased flexibility of the peptide that hinders haem orientation towards the electrode. On the whole, these properties make MKP a suitable starting material for engineering miniature haem systems of increasing complexity that, being characterized by good stability and electrochemical activity, might find applications in biosensor technology.

MATERIALS AND METHODS

Materials

Mp (Sigma Chemical Co., St. Louis, MO, U.S.A.) and *N*-succinimidyl-3-(2-pyridyldithio)propionate (SPDP; Sigma-Aldrich Chemical Co., St. Louis, MO, U.S.A.) were used without further purification. Peptide P21, purity more than 85 %, was synthesized on request by Peptide Products (Salisbury, Wilts., U.K.).

Basic methods

Spectrophotometric titrations were performed in phosphate buffer, pH 7.0, or in formate buffer, pH 4.5. A Cary 13 spectrophotometer (Varian) was employed for absorbance measurements. Reduction of the haem iron was obtained by adding a few grains of sodium dithionite.

CD spectra were recorded with a Jasco J-710 spectropolarimeter (Jasco, Tokyo, Japan) equipped with a personal computer as data processor. The molar ellipticity (degrees $\cdot$ cm^2 $\cdot$ dmol^{-1}) is expressed as $[\Theta]_M$ on a molar haem basis in the region 380–450 nm, and as mean residue ellipticity, $[\Theta]_{m.r.w.}$, in the far-UV region (mean residue molecular masses: Mp, 118; peptide P21, 84; MKP, 96).

Cyclic voltammetry measurements were performed with a PAR 273A potentiostat/galvanostat (PAR, Princeton, NJ, U.S.A.). Voltammograms were run in an anaerobic enviroment by removing O_2 from the electrochemical cell by a gentle flow of CO_2-free N_2, maintained just above the surface of the solution. A glassy carbon electrode (Metrohm, Henisau, Switzerland), 3 mm in diameter, was used for the voltammetric measurements; a saturated calomel electrode (Amel, Milan, Italy) was the reference electrode and the counter-electrode was platinum.

Sequencing was performed by automated Edman degradation on an Applied Biosystems model 470 A gas-phase sequencer equipped with an Applied Biosystem model 120 A phenylthiohydantoin analyser for the on-line identification of amino acid derivatives.

Chemical modification of Mp

Mp was dissolved in 50 mM phosphate buffer, pH 6.0, at a concentration of 0.5 mg/ml (260 μM). A 10-fold molar excess of SPDP dissolved in a minimum volume of DMSO was added to the solution and left to react for 1 h at room temperature; this reaction was expected to introduce the pyridyldithio group to the available amino groups of MP (Val-11 and Lys-13). The reaction was stopped by the addition of glycine (50 mM final concentration); the mixture was left for a further 1 h and then dialysed overnight against 50 mM phosphate buffer, pH 6.0, with size-selective membranes (Spectra/Pore 6 by Spectrum; 1000 Da cut off). Aliquots of the product were analysed by gel electrophoresis under native conditions [15]. The reacted samples showed increased mobility towards the cathode, indicating that the number of positive charges on Mp had decreased.

Cross-linking SPDP-Mp with the synthetic peptide P21

The synthetic peptide P21 was added to the modified SPDP-Mp at a 1.5:1 molar excess. The mixture was kept for 20 h at 4 °C under extensive dialysis against 50 mM phosphate buffer, pH 6.0, to favour the substitution of the SPDP pyridyldithio group with the free thiol group of Cys-1. After further dialysis against distilled water, the reaction mixture was stored or freeze–dried for purification.

Purification of Mp-P21 conjugates

Purification was performed with an HPLC apparatus (Pharmacia LKB, Uppsala, Sweden) equipped with a Uvicord UW2251 spectrophotometer and a personal computer as data recorder. After exploration of several conditions, the products of the reaction were purified from unconjugated Mp or P21 by ion-exchange chromatography or reverse-phase HPLC. Both techniques yielded similar results; however, ion-exchange chromatography failed to resolve the different reaction products satisfactorily when performed with a cation-exhange column (Q Sepharose Fast Flow; Pharmacia) at basic pH (pH 8.5). Under these conditions Mp tends to form aggregates, with a significant decrease in the degree of conjugation with P21. In contrast, reverse-phase chromatography, performed in the presence of 0.2 % trifluoroacetic acid, yielded satisfactory results because aggregation was prevented. The reaction mixture was applied either to a semi-preparative column (SPLC 8 Supelcosil; Supelco) or to a Pharmacia Resource P column equilibrated in 0.2 % trifluoroacetic acid; a linear gradient, starting from 30 % solvent B [70 % (v/v) CH_3CN/0.2 % trifluoroacetic acid], was run for 20 min (flow rate 3 ml/min) up to 80 % solvent B. Elution was monitored at 220 or 400 nm; the fractions obtained from different chromatographic runs were collected and pooled.

Computational methods

InsightII and Discover from MSI were used to model the cross-linking of Mp to P21. The molecular dynamics runs were performed at 300 K in the water droplet approximation, i.e. the complex was surrounded by a layer of 9.0 Å water molecules. Each molecular dynamics run was preceeded by 1000 steps of energy minimization with conjugated gradients of the starting complex. The simulation time ranged from 25 to 50 ps. Four trajectories were simulated that differed in the starting configuration of the complex or in the constrained distance between N_ζ of Lys-13 of Mp and S_γ of Cys-1 of P21.

RESULTS

Chromatographic and chemical analysis of the reaction products

Figure 2 shows a typical chromatogram of the reaction mixture obtained by the procedure described above. The solid line represents the elution profile monitored at 400 nm, which detects the absorbance of the haem; the broken line is the profile followed at 220 nm. Chromatography at 220 nm revealed the presence of five peaks, which are indicated as: peak 1 (retention time 2 min), assigned to unreacted Mp; peak 2 (retention time 2.7 min), assigned to P21; peak 3 (retention time 4.2 min), assigned to the main covalent complex, MKP; and peaks 4 (retention time 5.2 min) and 5 (retention time 6.4 min), also cross-linked products (see below). Fractions from the Resource P column were analysed by high-resolution reverse-phase chromatography on a C_{18} column (218TP from Vydac) and subjected to amino acid analysis and sequencing. Chromatography of Mp and P21 allowed the assignment of peaks 1 and 2. Our interest has been focused on peak 3, which was obtained in higher yield; the inset to Figure 2 illustrates the C_{18} profile of peak 3 obtained from the analytical column; at this resolution the purified MKP complex appears as a single species, with purity greater than 90%.

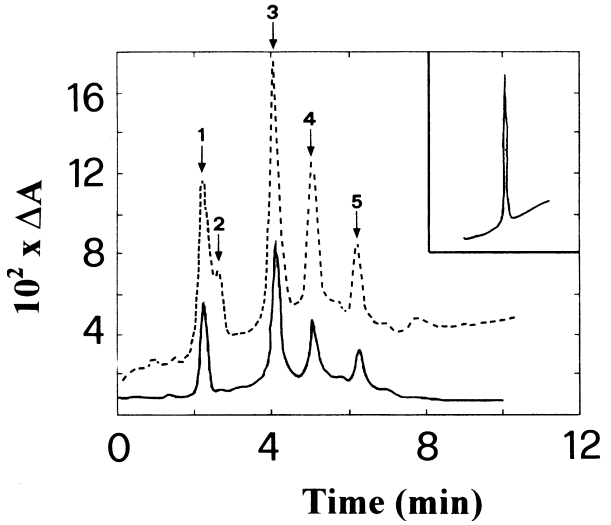

Figure 2 Chromatogram of the purification of MKP from the reaction mixture by reverse-phase HPLC semipreparative column (Resource P; Pharmacia) equilibrated in 0.2% trifluoroacetic acid

A linear gradient of 30–80% solvent B at a flow rate of 3 ml/min was used. The elution profile was monitored at 220 nm (broken line) or 400 nm (solid line). Arrows indicate the positions of the main peaks, which were identified as unreacted Mp (peak 1), unreacted P21 (peak 2), MKP (peak 3) and not characterized (peaks 4 and 5). The inset shows an analytical chromatography of the main reaction product (peak 3, MKP) obtained with a high-resolution reverse-phase C_{18} column (218TP from Vydac). Elution conditions were the same as for the Resource P column except that the flow rate was 1 ml/min.

Table 1 Amino acid composition of fraction 3 determined by HPLC chromatography (Figure 2)

Experimental data for MKP are compared with the known amino acid compositions of Mp and peptide P21.

	Composition		
Amino acid	MKP	Mp	P21
Asp	1		1
Thr	2.1	1	2
Ser	2.9		3
Glu + Gln	3	3	1
Ala	6.8	1	8
Val	1.4	2	
Leu	0.7		1
Phe	0.7		1
His	1.3	1	1
Arg	0.9		1
Lys	1.7	1	1

Peak 3 was shown to be MKP by chemical analysis; its amino acid composition (Table 1) shows that peak 3 is a 1:1 complex of Mp and P21 (see Figure 1). The same fraction was analysed by a protein sequencer; automatic Edman's degradation yielded the Val and Gln of Mp and stopped at Lys-13. This finding indicates that the covalent cross-link is between Cys-1 of P21 and Lys-13 of Mp. The amino acid compositions and partial sequences of two extreme fractions on the leading and trailing edges of peak 3 excluded the presence of contaminants.

Peaks 4 and 5 were not analysed extensively; however, a preliminary Edman degradation of peaks 4 and 5 suggested that in these cases the N-terminal Val of Mp was cross-linked to P21.

Binding of P21 to Mp

On addition of a solution of P21 to Mp, a co-ordination complex (presumably involving the imidazole group of His-13 and the haem iron) is quickly formed, as shown by optical spectroscopy. The binding of peptide P21 to Mp in phosphate buffer at pH 7.0, followed spectrophotometrically, is described by a hyperbola. The value of the apparent equilibrium constant (K_{eq}), as determined from the binding isotherm, is reported in Table 2, together with the equilibrium constants for the binding of imidazole and peptide P13 [14] to Mp. It can be noted that the dissociation constants of P13 and P21 are respectively one-fifth and one-sixth of that of imidazole. This confirms the hypothesis that (short-range) intramolecular interactions taking place as the peptide binds to Mp significantly stabilize the Mp–peptide complex.

Analysis of the optical spectra

Figure 3 shows the optical spectra of Mp, MKP and the Mp–imidazole complex, recorded in the Soret region (380–450 nm) at pH 7.0 (Figure 3A) and pH 4.5 (Figure 3B). The optical spectrum of the covalent complex MKP (with a maximum at approx. 407 nm) is very similar to those of Mp–imidazole and of the co-ordination complexes with P21 and P13 (results not shown) [14]. This finding supports the proposal that in the purified MKP complex, His-13 of P21 co-ordinates to the sixth

Table 2 Dissociation constants for the binding of imidazole, P13 and P21 to Mp

Experimental conditions: 0.1 M phosphate buffer, pH 7.0, or 0.1 M formate buffer, pH 4.5; temperature 25 °C. The results for P13 are taken from [14].

Ligand	pH	K_{eq} (M)
Imidazole	7.0	1.0×10^{-4}
	4.5	3.3×10^{-2}
P13	7.0	2.1×10^{-5}
P21	7.0	1.7×10^{-5}

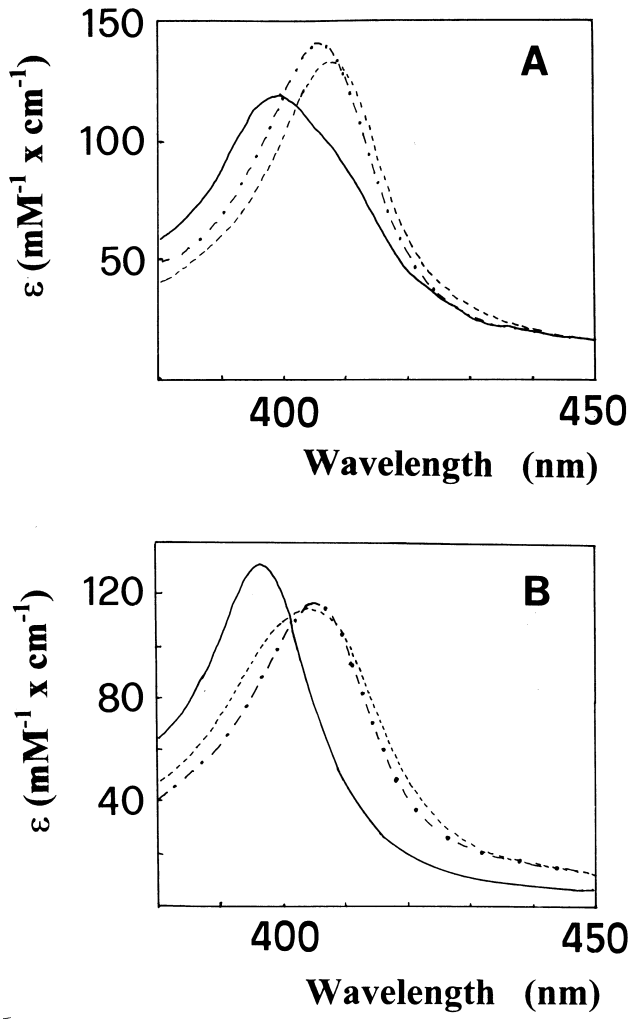

Figure 3 Absorbance spectra of Mp (solid line) MKP (broken line) and the Mp–imidazole complex (dot-dashed line) recorded in the Soret region (380–450 nm)

Experimental conditions: 50 mM phosphate buffer, pH 7.0 (**A**); 50 mM formate buffer, pH 4.5 (**B**); temperature 20 °C.

position of the haem iron in the Fe(III) state. Therefore MKP is co-ordinated to the metal, via His-13. Thus MKP can be viewed as a 'closed' complex, with P21 providing a number of additional possible contacts on the distal side, as inferred from the dissociation constant in Table 2.

By the pyridine–haemochromogen method [16], we have determined the molar absorption coefficients of Mp and MKP complex at acid pH; these are $\epsilon_{395} = 131.5 \pm 3.0\ mM^{-1} \cdot cm^{-1}$ and $\epsilon_{407} = 118.2 \pm 3.0\ mM^{-1} \cdot cm^{-1}$ respectively.

Replacement reaction by imidazole

The strength of the distal ligand–haem iron bond can be determined by replacement with another ligand competing for the same site. To estimate the free energy of binding of His-13 of P21 in the covalent complex MKP, we followed the displacement of axial His-13 as imidazole was added. It is important to point out that, although the optical spectra of Mp-imidazole and MKP are very similar (see Figure 3), they are not identical. In fact, the addition of a large excess (10 mM) of imidazole to MKP is associated with a spectral change in the Soret region, which can easily be detected by difference spectroscopy. Thus it is possible to titrate MKP with imidazole and follow the displacement reaction spectrophotometrically, as shown in Scheme 1, in which Im stands for imidazole.

From the optical titration (Figure 4) we can determine the apparent dissociation constant, K_d (obs), from K_{Im}/K_{His}. Given that His-13 is co-ordinated to the haem Fe(III) in the 'closed' configuration A but not in the 'open' configuration B, the equation can be applied if the dissociation constant of X (= imidazole) to configuration B and Mp is the same. As a matter of fact, from the molecular dynamics simulation (see below) the 'open' conformation leaves the sixth co-ordination position of the haem iron accessible to the solvent and we therefore assume that imidazole might have access to the haem iron without steric hindrance from P21. From the titration, a value of K_d (obs) = 19 mM at pH 7.0 is obtained for the concentration of imidazole necessary to shift the equilibrium from configuration A to BX in Scheme 1; given the value of 100 μM for K_{Im}, a value of 5.2 mM is calculated for K_{His}.

At pH 4.5, where imidazole is fully protonated, the same titration (see Figure 4B) yields a greater dissociation constant for the haem Fe(III), indicating a lower affinity for the haem iron [K_d (obs) = 0.1 M]. This is expected, given that the protonation state of imidazole ($pK = 6.95$) affects the formation of the complex between Mp and imidazole ($K_{Im} = 33$ mM at pH 4.5). Thus a value of 0.33 for K_{His} is obtained, showing a destabilization of the 'closed' configuration at pH 4.5 compared with pH 7.0.

CD measurements

CD measurements of the oxidized MKP complex were performed in the Soret (380–450 nm) and far UV (200–250 nm) regions, at neutral and acidic pH (i.e. pH 7 and 4.5). As illustrated in Figure 5 (upper panel), the Soret dichroic spectrum of the MKP complex shows a single, positive, band centred on approx. 408 nm, at both pH values; a broad shoulder at approx. 418 nm is observed only at acid pH. Under the same conditions, Mp displays a Soret dichroic spectrum strongly dependent on pH (results not shown); in particular, at neutral pH the spectrum displays a negative band centred on approx. 416 nm that, according to Urry [17], is indicative of the presence of aggregated material. Thus, similarly to the Mp–imidazole and Mp–P13 complexes [14], the absence of this negative band from the MKP spectrum indicates that this complex is monomeric.

The secondary structure of the complex was estimated by CD spectroscopy in the far UV (200–250 nm). As shown in Figure 5 (lower panel), MKP has an appreciable content of α-helical conformation at neutral pH (approx. 30%) [18]; in contrast, under the same conditions Mp is practically a random coil [14] and free P21 has a considerably smaller degree of α-helical

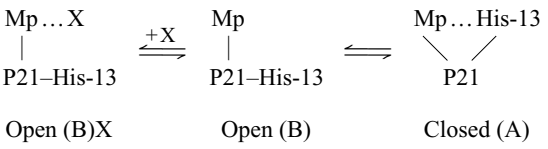

Scheme 1

X represents imidazole; the co-ordination bonds between His-13 or X and Fe(III) are indicated by dotted lines and the equilibrium constants for the two steps (K_{His} and K_{Im}) are expressed as follows: K_{His} = [B]/[A] and K_{Im} = ([B][X])/[BX], where Im stands for imidazole.

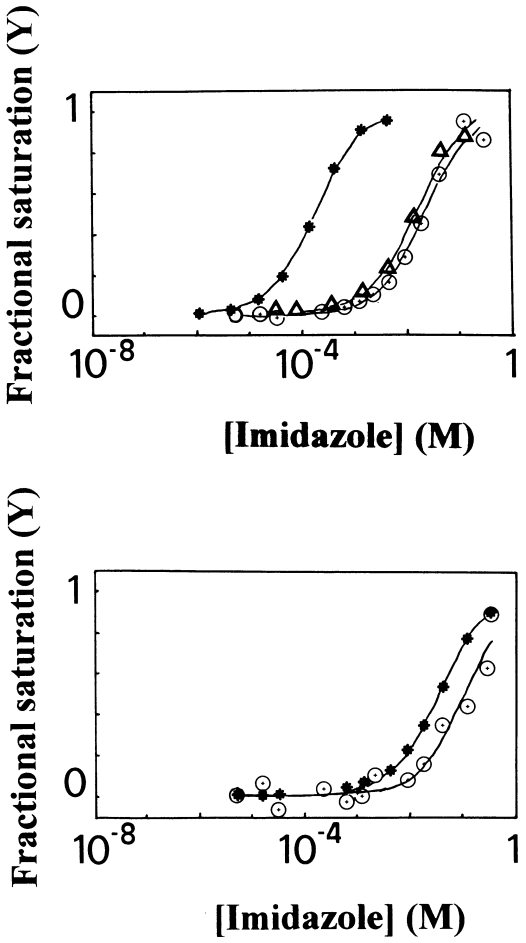

Figure 4 Titrations for the binding of imidazole to Mp (✱), Mp + P21 ([P21]$_t$ = 0.9 mM) (△) and MKP (⊙)

Upper panel, pH 7.0; lower panel, pH 4.5; experimental conditions were as described for Figure 3.

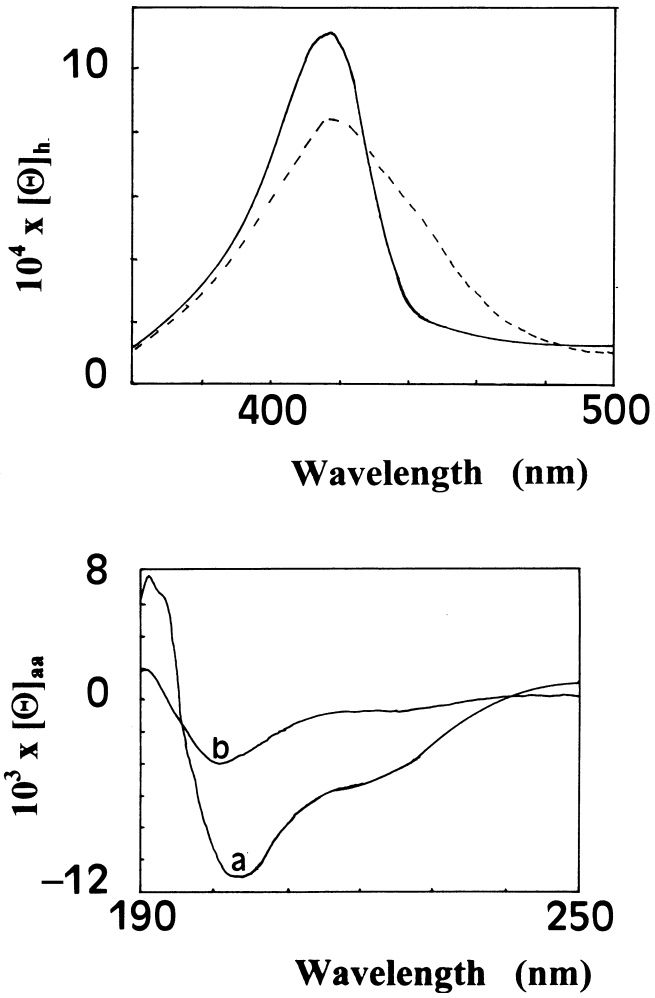

Figure 5 CD spectra of the MKP complex

Experimental conditions were as described for Figure 3. Upper panel: CD spectrum in the Soret (380–500 nm) region of MKP in 50 mM phosphate buffer, pH 7.0 (solid line), and 50 mM formate buffer, pH 4.5 (broken line), at 4 °C. Lower panel: far-UV CD spectrum of MKP in 50 mM phosphate buffer, pH 7.0 (a); CD spectrum in (b) is computed from data on the two separate components, i.e. Mp and peptide P21, and expected in the absence of conformational changes on complex formation. Abbreviations: $[\Theta]_h$, $[\Theta]_M$; $[\Theta]_{aa}$, $[\Theta]_{m.r.w.}$.

Table 3 Parameters for heterogeneous electron transfer of the MKP at a glassy carbon electrode

Experimental conditions: 50 mM formate buffer, pH 4.5, with 100 mM $NaClO_4$ as supporting electrolyte; temperature 4 °C. The scan rate for ΔE_p was 100 mV/s; $E_{\frac{1}{2}}$ values (±S.D.) are with respect to a normal hydrogen electrode. $E_{\frac{1}{2}}$ denotes the redox potential.

System	ΔE_p (mV)	$E_{\frac{1}{2}}$ (mV)
MKP	181 ± 5	43 ± 5
Mp	96 ± 5	11 ± 5
Mp–imidazole	71 ± 5	−14 ± 5

structure (results not shown). Thus, on complex formation, P21 increases its α-helical content significantly as shown clearly in Figure 5 (lower panel), where the dichroic spectrum of the complex is compared with that computed from the CD spectra of the two separate components. At acid pH (results not shown), the helix content of MKP is lowered.

Electrochemical activity

The voltammetric behaviour of the MKP complex has been investigated at pH 4.5 and low temperature, because these are the conditions that enhance the electrochemical activity of the complex. The direct-current cyclic voltammogram of the complex run with a glassy carbon electrode under the conditions specified in the legend of Table 3 shows a well-defined electrochemistry,

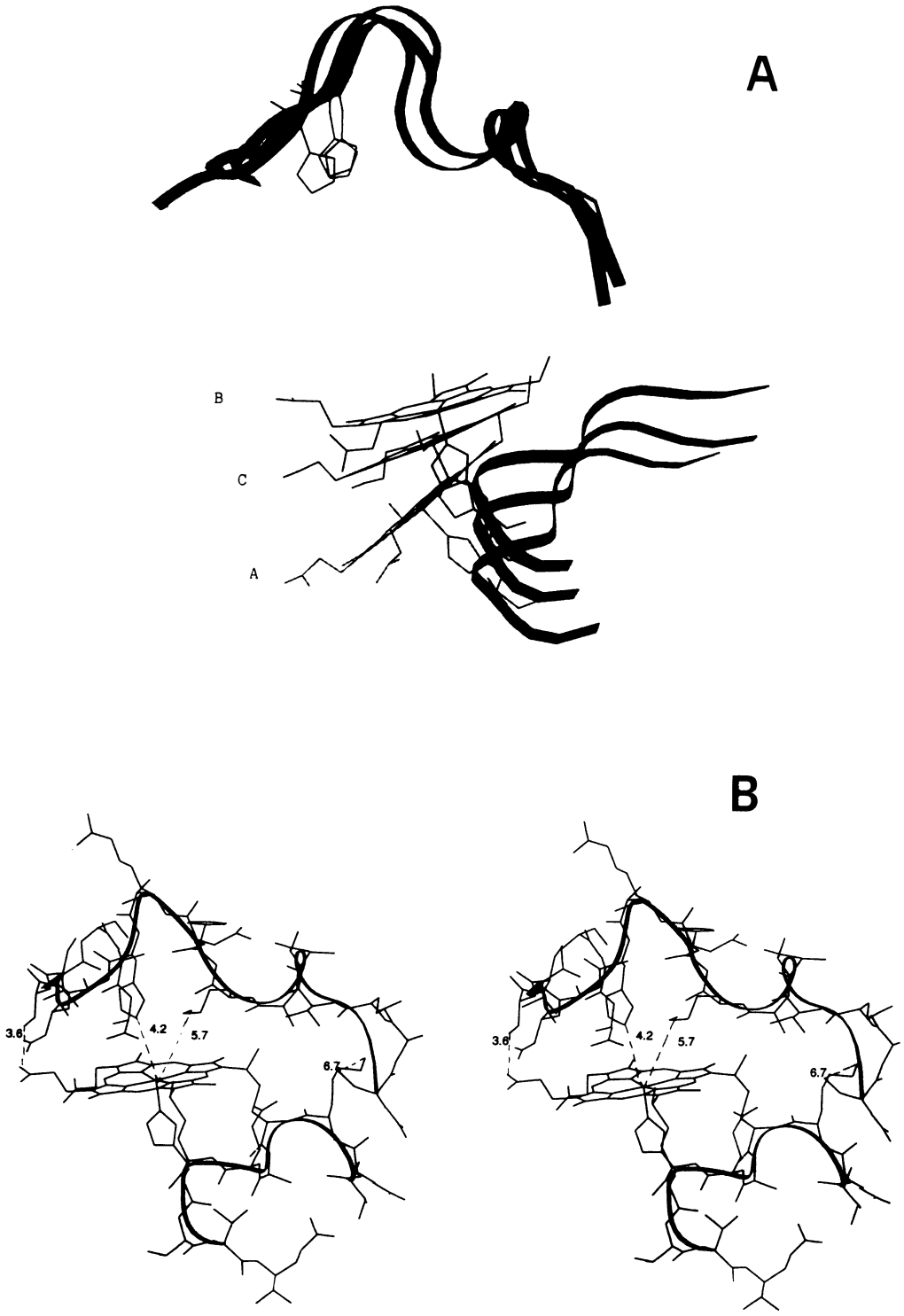

Figure 6 Molecular dynamics simulations of MKP

(**A**) Molecular dynamics simulation of the 'open' complex: the ribbons describe the backbone chains of the two peptides and only the haem is displayed. The three conformations refer to the starting configuration of the molecular dynamics run (A), to the last configuration recorded (B) and to the average configuration (C). The comparison is done by superimposing the backbone of P21: the displacement of the haem is roughly 6 Å. (**B**) Average conformation of MKP obtained in the molecular dynamics simulation of the 'closed' complex (stereo view). The reported average distances refer to N_{ζ} (Lys-8)–Fe, N_{δ} (His-13)–Fe and O_{γ} (Ser-17)–O (haem). The minimum and maximum distances for the axial ligands are respectively 4.7 and 6.4 Å for N_{ζ} (Lys-8)–Fe and 3.6 and 4.9 Å for N_{δ} (His-13)–Fe. The covalent cross-link between Mp and P21 is indicated at the right.

the cathodic and anodic peaks having similar magnitudes and the i_{pa}-to-i_{pc} ratio being close to unity. Furthermore the voltammetric peak currents vary with the square root of the potential scan rate, indicating that the process is diffusion-controlled [19]; the ΔE_p value calculated from the cyclic voltammogram (see Table 3) indicates that the redox process is quasi-reversible.

The redox potential, $E_{\frac{1}{2}}$, was estimated from the voltammograms (see Table 3). Examination of the results indicates that: (1) the redox potential of the MKP complex is more positive than that of the Mp–imidazole co-ordination complex by 50–60 mV, (2) compared with Mp, the redox potential shift is positive in MKP complex and negative in the Mp–imidazole complex, and (3) ΔE_p is significantly greater (by a factor 2) in the MKP complex, possibly indicating steric effects in the heterogeneous electron transfer process.

Molecular dynamics computation

To get a deeper insight into the structural features of MKP, we undertook a molecular dynamics simulation to define a suitable model fitting both the 'open' and 'closed' configurations of the complex. To this end, four molecular dynamics runs were performed with simulated trajectories differing in their starting complex configurations or in the constrained distances between the N_ζ of Lys-13 of Mp and the S_γ of Cys-1 of P21.

For the first two trajectories we assumed the 'open' complex as a starting configuration, with a structure average between those of the two isolated components and with no initial contacts (apart from the covalent cross-link between the two peptides). In these cases the two peptide chains moved one toward the other, the mean square displacement being 26 Å for Mp and 24 Å for P21. Figure 6(A) illustrates the peptides (as α-carbon ribbons) and the haem positions in the (A) starting, (B) final and (C) average configurations. Two residues, His-13 and Lys-8 of P21, compete for the sixth co-ordination position of the haem iron, although His-13 is favoured. Both simulations were followed starting with a His-13–Fe distance of approx. 20 Å, which reached a minimum of approx. 4 Å. The exposed haem surface seems to be solvated, although only one water molecule is co-ordinated to the iron atom at approx. 3.3 Å, characterized by an attractive interaction energy of -3.5 kcal/mol (-13.8 kJ/mol). Further, other solvent molecules are hydrogen-bonded to the polar side chains on the haem group.

In the other two simulations we assumed the 'closed' complex (the final configuration in Figure 6A) as the initial configuration: in one case we considered a constrained distance of 5 Å between the two cross-linked residues, Lys-13 of Mp and Cys-1 of P21, whereas in the second case no constraint was taken into account. The starting 'closed' structure was further minimized by conjugated gradients methods to reach a local energy minimum.

In both simulations the complex showed no tendency to fall back into an open configuration, the five snapshots taken during the dynamics (results not shown) being superimposable on one another. Figure 6(B) shows some interesting features of the simulated MKP complex: (1) the (previously exposed) haem surface becomes partly covered by P21, although the side bearing the two propionate groups remains largely exposed to the solvent and interacts with the side chain of the polar residues of P21 (mainly Ser-17 and Asp-15); (2) the competition between His-13 and Lys-8 of P21 for the distal position of the haem iron is evident but His-13 is significantly closer to the haem iron, its average distance being 4.29 Å with respect to the 5.69 Å of the positively charged Lys-8, which supports the hypothesis that His-13 is the prevailing axial ligand of the haem iron; and (3) no solvent molecules were observed within the haem pocket; further, the energy calculated for the Fe–N_ζ (Lys) and Fe–N_d (His) interaction was approx. -8 kcal/mol (-33.5 kJ/mol) at the minimal distance, i.e. approx. 3.6 Å.

DISCUSSION

Mp, the undecapeptide derived from the peptic hydrolysis of cytochrome *c*, is an interesting starting material for the construction of miniature haem complexes that might contribute to an understanding of the influence of the protein matrix on the reactivity of the haem. We recently described the characterization of the complex obtained by binding to Mp a synthetic analogue of the C-peptide (residues 1–13) of RNase A (peptide P13; [14]), which probably co-ordinates to Fe(III) of Mp at the axial position via the imidazole group of a histidine residue. At neutral pH, the complex was shown to possess appreciable thermodynamic stability, a good propensity for acquiring α-helical structure at low temperature and satisfactory electrochemical activity; further, unlike Mp, it is monomeric under the conditions investigated.

In the present paper we report the synthesis, purification and characterization of a covalent complex obtained by cross-linking Mp to a synthetic 21-mer (P21) with a sequence closely resembling that of the S-peptide (residues 2–21) of RNase A. P21 can be cross-linked to Mp to form a stable complex characterized by a secondary structure and appreciable electrochemical activity. The covalent complex MKP is obtained by the formation of a disulphide bond between Cys-1 of P21 and Lys-13 of Mp, previously modified with a thiol-introducing compound (i.e. SPDP; see the Materials and methods section). From the reaction mixture, a product with purity greater than 90% is obtained after HPLC purification. An amino acid composition analysis as well as a partial sequence analysis both showed that MKP is formed by Mp and P21 in a 1:1 molar ratio (see the Introduction section). Weak reductants do not reduce MKP; however, strong reductants, such as sodium dithionite, cause the rupture of the complex into its components, which makes investigations of its reduced state difficult.

It is known that Mp aggregates at neutral pH, possibly via Lys-13, which co-ordinates to the haem iron of another Mp molecule [17]; however, the addition of imidazole strongly decreases aggregation because this compound competes with Lys-13 for the sixth co-ordination site of the haem iron. In this paper we have shown that MKP is a monomer stabilized by the co-ordination of His-13 of P21 to the haem iron of Mp, as shown by absorption and CD spectroscopies. Data in the far UV indicate that, at pH 7.0 and 4 °C, MKP has an appreciable α-helical content (approx. 30%), unlike Mp, which is mostly randomly coiled, and peptide P21, which is poorly structured. Thus on complex formation a significant number of residues (three or four) acquire secondary structure, indicating that complexing increases the order parameter of the molecule.

Acid pH seems to enhance the redox behaviour of the MKP complex; under these conditions, the system displays quasi-reversible electrochemical activity at a glassy carbon electrode. It should be noted that at acidic pH, where the protonated His-13 of P21 does not bind the haem iron ('open' conformation) the P21 is still interacting with Mp, as indicated by the molecular dynamics simulation. However, the flexibility of P21 in the 'open' conformation could leave the electrode surface accessible to the haem moiety. In contrast, at neutral pH, when MKP is in the 'closed' conformation, P21 inhibits electron transfer between the electrode and iron, possibly by hindering the haem moiety or by not allowing a proper orientation of MKP towards the electrode. Interestingly, the redox potential of MKP is positively

shifted with respect to Mp, whereas the Mp–imidazole complex is characterized by a more negative redox potential. This could be assigned, at least in part, to steric effects occurring in MKP; because the haem surface accessible to the solvent in MKP is decreased, the redox potential is shifted towards the value of the parent macromolecule cytochrome *c*.

Further analysis of data shows some interesting features. The equilibrium constants reported in Table 2 indicate that peptide P21 co-ordinates to Mp with higher affinity than imidazole; such a finding confirms the hypothesis presented previously [14] that claims a significant area of contact involving short-range interactions between residues of the two peptides and the haem group in the complex. It seems from our results that the larger that the area of contact is, the greater is the stability of complex. The strength of the co-ordination bond between His-13 of P21 and the haem iron in MKP has been estimated through displacement with imidazole, which is known to co-ordinate to the iron. The displacement reaction has been followed by optical spectroscopy, the co-ordination of imidazole to Mp and to MKP yielding similar but not identical spectra (see Figure 3). Results at neutral pH indicate that the affinity of imidazole for Mp is approx. 190-fold that for MKP; at pH 4.5 protonated imidazole binds to the haem iron very weakly, so in these conditions the His-13–Fe(III) bond is weaker and the 'closed' conformation is destabilized.

We have proposed a simple model predicting that MKP is an equilibrium mixture of 'open' and 'closed' conformations, the latter being stabilized by a co-ordination bond between Fe(III) and His-13 of P21, and some additional interactions between the peptide side chains. The equilibrium constant between the 'open' and the 'closed' conformations of MKP at pH 7.0 is approx 0.005. This can be further interpreted on the basis of results obtained by molecular dynamics simulation, which indicate how the co-ordination of His-13 of P21 to Fe(III) is partly weakened both by Lys-8 (a residue that competes for the same site) and by the structural tensions due to the short-range interactions between residues of the C-terminal side of P21 and residues of Mp (such as the hydrogen bond between Ser-17 of P21 and and one of the haem propionate groups), which significantly increase the structural rigidity of the complex. These events seriously contrast optimization of the His-13 co-ordination at the axial position of the haem iron.

Received 18 April 1997/12 August 1997; accepted 13 August 1997

These simulations suggest that a modified P21 with specific substitutions at position 8 should lead to the enhanced stability of the 'closed' conformation. Moreover we are able to design additional peptides with specific functions and/or optical probes to investigate the dynamics of binding of His-13 to the haem iron of Mp on the collapse of the covalent P21 peptide from the 'closed' conformation. These studies are in progress.

We thank V. Abruscato, who contributed to running the molecular dynamics simulations, and Professor D. Barra for the amino acid analysis and N-terminal sequence of MKP. This work is part of the National Project of Research on Technologies for Bioelectronics funded by the Italian Ministry for University and Scientific and Technological Research (MURST) and assigned to Pharmacia & Upjohn as main contractor.

REFERENCES

1 Moser, C. C., Keske, J. M., Warncke, K., Farid, R. S. and Dutton, P. L. (1992) Nature (London) **355**, 796-802
2 Harbury, H. A. and Loach, P. A. (1959) Proc. Natl. Acad. Sci. U.S.A. **45**, 1344–1359
3 Harbury, H. A. and Loach, P. A. (1960) J. Biol. Chem. **235**, 3640–3645
4 Santucci, R., Reinhard, H. and Brunori, M. (1988) J. Am. Chem. Soc. **110**, 8536–8537
5 Wilson, M. T., Ranson, R. J., Masiakowski, P., Czarnecka, E. and Brunori, M. (1977) Eur. J. Biochem. **77**, 193–199
6 Kimura, K., Peterson, J., Wilson, M., Cookson, D. J. and Williams, R. J. P. (1981) J. Inorg. Biochem. **15**, 11–25
7 Ayasaka, N., Kondo, T., Kido, M. A., Nagata, E. and Tanaka, T. (1992) Arch. Oral Biol. **37**, 363–369
8 Brunori, M., Santucci, R., Campanella, L. and Tranchida, G. (1989) Biochem. J. **264**, 301–304
9 Santucci, R., Faraoni, A., Campanella, L., Tranchida, G. and Brunori, M. (1991) Biochem. J. **273**, 783–786
10 Bierzynski, A., Kim, P. S. and Baldwin, R. L. (1982) Proc. Natl. Acad. Sci. U.S.A. **79**, 2470–2474
11 Mitchinson, C. and Baldwin, R. L. (1986) Proteins **1**, 23–33
12 Shoemaker, K. R., Kim, P. S., York, E. J., Stewart, J. M. and Baldwin, R. L. (1987) Nature (London) **326**, 563–567
13 Kim, P. S. and Baldwin, R. L. (1984) Nature (London) **307**, 329–334
14 Santucci, R., Picciau, A., Antonini, G. and Campanella, L. (1995) Biochim. Biophys. Acta **1250**, 183–188
15 Davis, A. (1964) Ann. N.Y. Acad. Sci. **121**, 404–408
16 Paul, K. G., Theorell, H. and Akeson, A. (1953) Acta Chem. Scand. **7**, 1284–1287
17 Urry, D. W. (1967) J. Am. Chem. Soc. **89**, 4190–4196
18 Greenfield, N. and Fasman, G. D. (1969) Biochemistry **8**, 4108–4116
19 Nicholson, R. S. and Shaim, I. (1964) Anal. Chem. **36**, 706–723